

Distance Measurements between ¹³C Nuclei in Singly Labeled *p*-Xylene/Dianin's Inclusion Compound by 2D-RFDR

Eduardo Zaborowski,^{*1} Herbert Zimmermann,[†] and Shimon Vega^{*2}

^{*}Department of Chemical Physics, Weizmann Institute of Science, Rehovot, Israel; and

[†]Max-Planck-Institut für Medizinische Forschung, Heidelberg, Germany

Received April 6, 1998; revised September 1, 1998

Two-dimensional magnetization exchange experiments, with the radio-frequency-driven recoupling pulse sequence in the mixing time, have been performed for the detection of homonuclear ¹³C–¹³C distances between the singly ¹³C labeled methyl carbon of *p*-xylene and the natural abundant ¹³C nuclei of the host molecules in *p*-xylene/Dianin's complex. The intensities of the cross peaks between the methyl carbon and six host carbons were measured as function of the length of the mixing time and normalized by the intensities of their diagonal peaks. The results were compared with simulations based on the known distances in the complex. Good agreement was obtained, without taking the homonuclear zero-quantum linewidth ($1/\pi T_2^{ZQ}$) into account. This can be understood by realizing that in this complex the ¹³C carbon pairs are significantly diluted. © 1999 Academic Press

Key Words: dipolar interaction; RFDR; natural abundant carbons; homonuclear ¹³C distances; Dianin's compound.

INTRODUCTION

The internuclear magnetic dipolar interaction is a rich source of structural information in solids and liquids (1). Recently, solid state NMR techniques have been introduced that make use of this interaction to measure internuclear distances (2–14). Almost all these techniques require a combination of sample spinning (MAS) and synchronously applied radiofrequency (rf) pulses. For distance determinations between heteronuclear spins the most commonly used technique is the rotational echo double resonance (REDOR) experiment (12), while for homonuclear spin pairs the rotational resonance (R²) method should in particular be mentioned (2). In the REDOR method, dipolar dephased signals $S(t)$ are compared with nondipolar dephased signals $S_0(t)$ in the form $(S_0(t) - S(t))/S_0(t)$ (12). This enables the elimination of relaxation effects on the results and makes an accurate nuclear distance measurement possible. In the case of a homonuclear ¹³C–¹³C interaction the magnetization exchange R² experiment on a high abundant spin pair is unique in the sense that it does not require rf pulses during the

dipolar dephasing of the signals $S(t)$. Generally, however, it is necessary to account for the zero-quantum relaxation time T_2^{ZQ} of the coupled spin pair in order to deduce a nuclear distance from the pure dipolar decay $\exp(t/T_2^{ZQ})S(t)$. According to the work of Griffiths *et al.* (15), in which they apply the rf-driven dipolar recoupling (RFDR) technique to measure distances in bacteriorhodopsin, the zero-quantum relaxation time governing the homogeneous zero-quantum line broadening of a pair of high abundant coupled spins is mainly dependent on the homonuclear dipolar interactions between the spin pairs in the crystal and between the natural abundant spins and the spin pairs themselves. The first can be partially overcome by isotopic dilution of the spin pairs in the solid. However, the natural abundant ¹³C nuclei present in the sample are not easily removed. Molecular motions can also modify the zero-quantum line broadening. To overcome the need for the T_2^{ZQ} determination Costa *et al.* recently introduced the rotational resonance tickling experiment (16). In addition to the static and dynamic effects influencing the experimental T_2^{ZQ} values, insufficient heteronuclear decoupling and pulse imperfections can also change the dipolar decay signals $S(t)$ (2, 15, 17). Here we should mention that variations in the chemical shift parameters can have a significant influence on the R² signal dephasing (2).

Knowledge about the same zero-quantum relaxation time is also required in the simple rf-driven recoupling RFDR experiments on ¹³C-spin pairs (5). In these experiments, after spin excitation by cross polarization and selective inversion of one spin, π pulses are applied once each rotor cycle to the spin pair (the SEDRA sequence (18)) during high-power proton decoupling. While the R² experiment is very sensitive to the exact setting of the spinning speed (it must be equal to an integer multiple of the difference between the isotropic chemical shifts of the spin pair), RFDR is not. RFDR can in fact be considered as a frequency-broadened R² experiment. The experimental results of both dephasing techniques are dependent on T_2^{ZQ} and on residual heteronuclear interactions when the decoupling is insufficient. In the RFDR case they can also be influenced by pulse imperfections and cross polarization during these pulses (15–17). Although the signal dephasing in R² and RFDR is dependent on the magnitudes of the chemical shift anisotropies

¹ Current address: Department of Molecular Biology, The Scripps Research Institute, La Jolla, CA.

² To whom correspondence should be addressed.

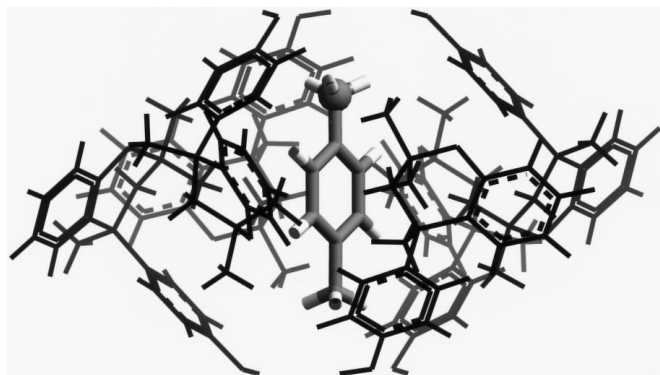


FIG. 1. One cage of the *p*-xylene/Dianin's inclusion compound. The guest *p*-xylene molecule is visible at the center of the cage, and the ^{13}C -labeled methyl carbon is pictured as a ball.

of the spins and their relative orientations with respect to the internuclear vector, we should expect that RFDR is less influenced by chemical shift changes than R^2 .

In this publication we report RFDR experiments on ^{13}C – ^{13}C pairs in a singly labeled inclusion compound where the carbon pair density is low (the smallest average distance between two labeled ^{13}C is about 8 Å), and the distances between the carbons in a pair are larger than 4 Å (without the presence of intermediate carbons). This is accomplished by inclusion of singly labeled *p*-xylene molecules at one of the methyl positions in the void cages of Dianin's compound. These methyl carbons do not experience any significant molecular motion (19). In this case we expect the value of T_2^{ZQ} to be large and, as will be shown, the experimental RFDR decay signals of the natural abundant host ^{13}C nuclei to provide nuclear distances.

Two-dimensional magnetization exchange experiments, with the RFDR sequence in the mixing time, is commonly used for the detection of carbon–carbon proximities in isotopically enriched samples (5, 15). After generation of ^{13}C transverse magnetization by cross polarization from protons and an evolution time t_1 , a $\pi/2$ pulse flips the magnetization back to the z direction just before the mixing period. During this period of length τ , the SEDRA sequence is applied and at the end an additional $\pi/2$ pulse rotates the magnetization to the xy plane where the signal is acquired during the detection time t_2 . Double Fourier transformation of the data results in diagonal and cross peaks between the isotropic chemical shifted lines of the interacting nuclei as in liquid state NOE spectra (1). The τ dependence of the cross-peak amplitudes can, in principle, be used to estimate internuclear distances. Although these 2D experiments are in most cases applied on uniformly enriched samples, they can of course also be applied to single spin pairs. In this study we apply 2D-RFDR on single spin pairs in order to determine nuclear distances. The reason for doing so is first that by singly ^{13}C labeling a set of distances can be detected simultaneously between this carbon and its neighboring natural

abundance carbons. Second, the diagonal peaks in the 2D spectrum can be used as a signal intensity reference for the determination of these distances, while partially eliminating the effects of relaxation and experimental parameters influencing the cross-peak intensities. When the natural abundant carbon spectra can be obtained and show enough spectral resolution, this approach can be useful in particular when distances of the order of 4–6 Å are monitored.

The 2D-RFDR experiments have been performed on a singly ^{13}C labeled *p*-xylene/Dianin's inclusion compound. Dianin's compound (4-*p*-hydroxyphenyl-2,2,4-trimethylchroman) is an organic clathrate, in which a large variety of small molecules can be included (20). In Dianin's inclusion compound six host molecules from an hourglass-shaped cage. The ends of each cage are formed by six hydrogen-bonded hydroxyl groups, which belong to six host molecules successfully pointing up and down with respect to the plane of the hexagonal OH ring. The inclusion compound with *p*-xylene contains one guest molecule per host cage, as is visualized in Fig. 1.

The room temperature ^{13}C NMR spectrum of the labeled *p*-xylene/Dianin's inclusion compound is shown in Fig. 2, together with the chemical structure of Dianin's molecule and the assignment of the host molecule carbons, following the work of Barker *et al.* (21) and our recent study of this inclusion compound by solid state NMR and molecular modeling (22).

In the next section we describe the details of the experimental procedures. Then the theoretical aspects of our RFDR calculations and results of the 2D-RFDR are presented, followed by the analysis of the data.

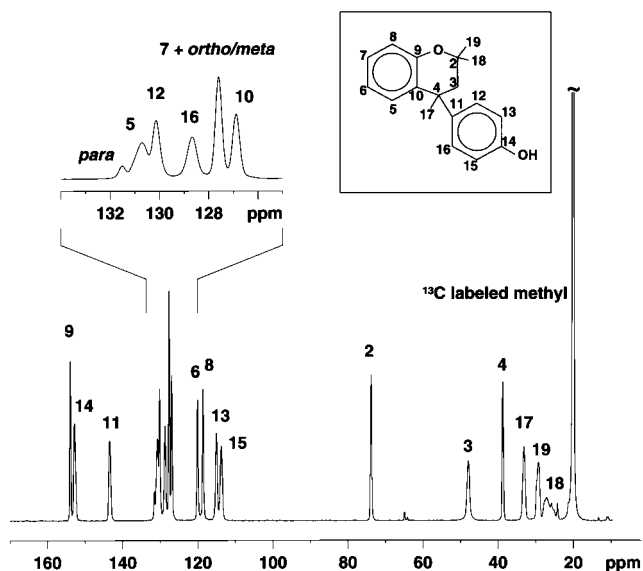


FIG. 2. The chemical structure of Dianin's compound, and our assignment of the ^{13}C MAS NMR spectrum at room temperature. The ^{13}C -labeled methyl line is truncated.

MATERIALS AND EXPERIMENTAL

The *p*-xylene/Dianin’s inclusion compound was prepared by recrystallization of the guest-free Dianin’s compound first from a solution of unlabeled *p*-xylene and then from a solution of *p*-xylene, specifically ¹³C labeled at one of the methyl positions (99% ¹³C, referred to henceforth as labeled *p*-xylene).

¹³C NMR spectra were recorded on a Bruker DSX-300 AVANCE spectrometer at a frequency of 75.47 MHz, using a BL 4-mm Bruker MAS probe. The spinning speed was controlled by the Bruker Pneumatic Unit with an accuracy of ±2 Hz. Variable amplitude cross-polarization (VACP) sequences were used to generate ¹³C magnetization, with a proton rf irradiation field of 86.2 kHz ($\pi/2$ pulse = 2.9 μ s) and a CP contact time of 4 ms. Proton decoupling, with the same rf intensity, was accomplished with the two-pulse phase-modulated (TPPM) scheme (23). The 2D-RFDR spectra were acquired with a rotating speed of $\omega_R = 6200$ Hz. The rf field in the carbon channel was 55.6 kHz for the $\pi/2$ pulses (4.5 μ s) and 28.9 kHz for the recoupling π pulses (17.3 μ s). The lower power (one-third of the Hartman–Hahn matching condition) of the recoupling pulses is crucial in order to minimize the effects of cross polarization to protons during the mixing time (24). The recoupling pulses applied during the mixing time, which varied between 16 and 96 rotor cycles (2.5–15.5 ms approximately), were given according to the XY-16 scheme in order to diminish the effects of pulse imperfections and of resonance offsets in echo formations (25). The spectral width was 240 ppm in both ω_1 and ω_2 dimensions. Sixteen scans were accumulated for each of the 256 t_1 steps, with a 4-s delay between scans. 2D phase sensitive spectra were obtained with the TPPI method, and 2048 × 512 points spectra were generated. All chemical shifts were referred by setting the glycine carboxyl resonance line at 176.04 ppm.

THEORY AND SIMULATIONS

Simulations of the carbon spectra were carried out with a FORTAN program that takes into account all necessary experimental parameters, such as sample rotation frequency, isotropic and anisotropic chemical shift parameters, dipolar interaction strengths, pulse lengths, timings, and rf field strengths. The chemical shift anisotropy (CSA) tensor parameters of all carbons were estimated, using typical values reported by Duncan (26). The distances between the ¹³C-labeled carbon of the guest methyl group and the host carbons were derived from X-ray data as described in Ref. (22). In Table 1 the CSA parameters and nuclear distances used in this study are summarized.

To determine the nuclear distances we performed TPPI 2D-RFDR experiments for different mixing times τ . To analyze the data we first calculated the 1D-RFDR dephasing curves for the different host–guest, *S* and *I*, respectively, carbon pairs. For these simulations the *S*-spin signals $S(\tau)$ were

TABLE 1
Chemical Shift Anisotropy Tensor Components and Nuclear Distances (between Host Carbons and the Guest *CH₃) Considered in the Simulations

	σ_{xx} (kHz)	σ_{yy} (kHz)	σ_{zz} (kHz)	Host carbon	<i>r</i> (to *CH ₃) (Å)
Guest *CH ₃	0.3	1.0	−1.3	—	—
Aliphatic quaternary	0.0	0.2	−0.2	C1	5.5
Aromatic C–H	1.7	6.2	−7.9	C13	4.4
				C15	4.7
				C16	5.3
Aromatic C–	2.0	6.6	−8.6	C11	5.7
				C14	4.1

evaluated by calculating the expectation values of the lowering operator S^- after the application of an RFDR pulse sequence of length τ on the initial state I_Z of the carbon pair in a set of single crystallites. We assumed the initial signal intensities of the carbons in the *I*–*S* spin pair to be equal. The time-dependent *S*-spin signal of a single crystallite, with a CSA tensor orientation defined by the Euler angle (α, β, γ) in the rotor frame, after the RFDR sequence can be expressed as (27)

$$S(\tau) f^*(\gamma) f(\omega_R t + \gamma), \quad [1]$$

where $f(\omega_R t) = \sum_n d_n e^{in\omega_R t}$ is the signal for $\gamma = 0$ due to the CSA interaction only, and $S(\tau)$ is a function that oscillates between 0 and 1 with an RFDR frequency, that is, a function of all dipolar, CSA, and pulse parameters (28). A zero isotropic chemical shift value is assumed. The RFDR signals are obtained by integration over all angles $\Omega = (\alpha, \beta, \gamma)$ on a sphere (powder signal) and can be evaluated and expanded as

$$R(\tau, t) = \int S(\tau) f^*(t) f(\omega_R t + \gamma) d\Omega = \sum_n I_n(\tau) e^{in\omega_R t}, \quad [2]$$

where $I_n(\tau)$ are the center and sideband intensities of the powder MAS spectra. After the mixing time τ , the value of this function (at $t = 0$) gives the total intensity of the *S*-spin spectrum and varies from 0 to $\frac{1}{2}$.

1D-RFDR buildup curves $R(\tau, t)$ of the *I*–*S* spin pairs were simulated for single crystallites, and powder signals were obtained by integration with the method of Cheng *et al.* (29).

The nuclear distances considered in this publication are all larger than 4 Å, resulting in dipolar interactions smaller than 120 Hz. To check the sensitivity of the RFDR curves $R(\tau, 0)$ on changes in the relative orientations of the chemical shift and dipolar tensors, we performed a set of simulations by varying the Euler angles of one of the CSA tensors and the polar angles of the dipolar vector. In our experiments one of the spins (the labeled methyl guest carbon) has a very small CSA tensor,

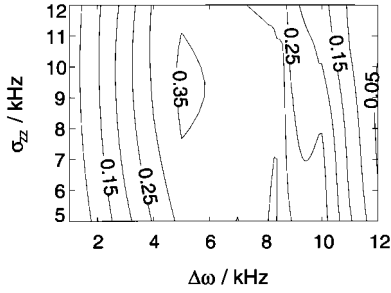


FIG. 3. Contour plot of the dipolar recoupling of a spin pair as a function of the difference between their off-resonances and of the highest component σ_{zz} of the CSA tensor (η constant, 0.65) of one of the spins (S). The simulation was performed starting with a z -magnetization of one spin (I), and monitoring the growth of the magnetization of the other spin (S) after a RFDR mixing time of 96 rotor cycles, for a dipolar coupling of 100 Hz, spinning speed of 6200 Hz, $H_1(^{13}\text{C})$ of 28.9 kHz for the recoupling π pulses, and a chemical shift anisotropy for the S spin as given in Table 1.

while the other spin can have CSA parameters according to Table 1. For some typical isotropic chemical shift differences $\Delta\omega$ and spinning speeds $2\Delta\omega > \omega_R > 0.5\Delta\omega$ and with dipolar interactions smaller than 120 Hz these simulations indicate that the asymmetry parameter of the host carbon tensors (η_{CS}), the relative orientation of the host and guest carbon CSA tensors, and the relative direction of the dipolar vector connecting the I and S nuclei do not influence the magnitude of the 1D-RFDR results by more than 2–3%: In our simulations we therefore considered only the CSA and isotropic chemical shifts of the host carbons and the strength of the dipolar interaction. The dependence of $R(\tau, 0)$ on the CSA and $\Delta\omega$ parameters, while keeping the spinning speed ($\omega_R = 6.2$ kHz) and the anisotropy of the tensor ($\eta_{\text{CS}} = 0.65$) constant, is demonstrated in Fig. 3. A contour plot of $R(\tau, 0)$ for $\tau = 15.5$ ms as a function of the largest component of the CSA tensor (σ_{zz}) and of the isotropic chemical shift difference $\Delta\omega$ is shown. Very little dependence on the CSA tensor strength, especially when σ_{zz} is in the range 8–11 kHz, is observed. The major dependence is clearly on the isotropic chemical shift difference showing maximum $R(\tau, 0)$ values close to the rotational resonance condition.

The τ dependence of the RFDR signal, corresponding to $R(\tau, 0)$, can be obtained by measuring the S -spin signal immediately after the RFDR pulse sequences or by monitoring the intensities of the centerbands after Fourier transformation, $I_0(\tau)$. A set of simulations for the various CSA, $\Delta\omega$, and ω_R values, relevant for our host–guest carbon pairs and with a dipolar interaction smaller than 120 Hz, have shown that the differences between the two methods of detection is not more than 3%. This is even so for the largest CSA tensor parameters in Table 1.

The τ -dependence of the intensities of the diagonal and cross peaks in the 2D-RFDR spectrum can also be estimated using the expressions in Eqs. [1] and [2]. Assuming that the host S -spin is on-resonance and the guest I -spin, with zero CSA

parameters, is at an off-resonance value equal to $\Delta\omega$, the signal of a ^{13}C -spin pair in a single crystallite at t_1 is given by

$$a(f^*(\gamma)f(\omega_R t_1 + \gamma) + e^{i\Delta\omega t_1}), \quad [3]$$

where we assumed that the initial amplitudes a of the two spins are equal.

Because of the TPPI phase cycling scheme, only the real part is detected:

$$a[\text{Re}\{f^*(\gamma)f(\omega_R t_1 + \gamma)\} + \cos \Delta\omega t_1]. \quad [4]$$

If we ignore the effect of the zero-quantum relaxation time T_2^{ZQ} , the powder t_2 -signal of a natural abundant (NA) S -spin carbon in the spin pair can be expressed and expanded as

$$\begin{aligned} & \int a\{\text{Re}\{f^*(\gamma)f(\omega_R t_1 + \gamma)\}(1 - S(\tau)) + \cos \Delta\omega t_1 S(\tau)\} \\ & \quad \times f^*(\omega_R t_1 + \gamma)f(\omega_R(t_1 + t_2) + \gamma)d\Omega \\ & = \sum_{n,m} \{F(n\omega_R, m\omega_R) + F(\Delta\omega + n\omega_R, m\omega_R)\} e^{in\omega_R t_1} e^{im\omega_R t_2}. \end{aligned} \quad [5]$$

Numerical powder integration of Eq. [5] is necessary to obtain the exact intensities of the center and sidebands in the spectrum. However, according to the 1D-RFDR calculations we can assume that it is sufficient for our spin pairs to restrict ourselves to the detection of the ratios between the powder cross peak centerband $F_0(\Delta\omega, 0)$ and the diagonal peak centerband $F_0(0, 0)$. By considering this ratio, we expect to compensate for two effects: the lack of knowledge on the actual intensities of the cross peaks at large RFDR mixing times and the effects caused by pulse imperfections. Thus,

$$\frac{F_0(\Delta\omega, 0)}{F_0(0, 0)} = \frac{R(\tau, 0)}{1 - R(\tau, 0)}. \quad [6]$$

This will be valid when the magnitudes of the CSA components are of the order of the spinning speed or smaller and the dipolar interaction is small. The validity of this expression for large dipolar interactions and CSA values much larger than the spinning speed still has to be examined. An extended study of the τ -dependence of the center and sideband intensities in the 2D-RFDR spectra is necessary in order to find the experimental parameters for which this approach is exactly valid. In particular, the sidebands that are present because of the TPPI phase cycling can make the data analysis complicated. The time-reversal TPPI experiment can improve the analysis, by elimination of sidebands and the pure absorption lineshapes in the 2D spectra (30). In the next section we discuss our 2D-RFDR

results of the ¹³C-spin pairs in the *p*-xylene–Dianin’s compound. The experimental values of the ratio in Eq. [6] are in principal dependent on the zero-quantum relaxation time. However, we will show that for our spin system the agreement between experimental and theoretical results, following Eq. [6], is reasonable.

RESULTS AND DISCUSSION

The pulse scheme for the 2D-RFDR experiment is given in the bottom part of Fig. 4. In the top part of Fig. 4, we show the 2D-RFDR spectrum obtained for a mixing time of $96T_R \approx 15.5$ ms. The off-diagonal sideband patterns described previously are clearly seen, as well as the cross peaks between the host and guest lines. The ω_2 slice at the resonant frequency ω_1 of the guest-labeled methyl carbon is shown at the top of the 2D spectrum. In Fig. 5 we show the 70- to 160-ppm region of τ -dependent ω_2 spectra at the ω_1 chemical shift of the ¹³C-labeled methyl guest carbons in the RFDR-2D spectra. The constant ω_1 slices were used because they had a better *S/N* than the constant ω_2 slices. The stack plot shows the growth of the cross peaks as a function of τ , from a short (a) $\tau = 1.5$ ms to a long (e) $\tau = 15.5$ ms mixing time. We analyzed only those

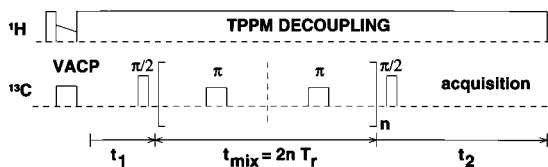
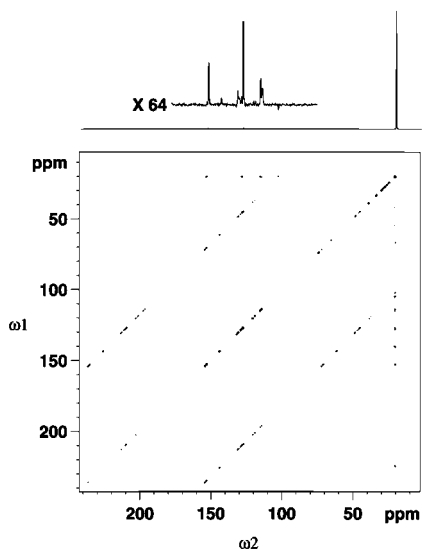


FIG. 4. The 2D-RFDR pulse sequence (below) and the spectrum obtained for a mixing time of $96T_R \approx 15$ ms. The off-diagonal sideband patterns are a consequence of the TPPI scheme used for the 2D data collection. The ω_2 spectrum at $\omega_1 = 20$ ppm (cross peaks of the ¹³C-labeled methyl carbon) is shown at the top of the 2D spectrum.

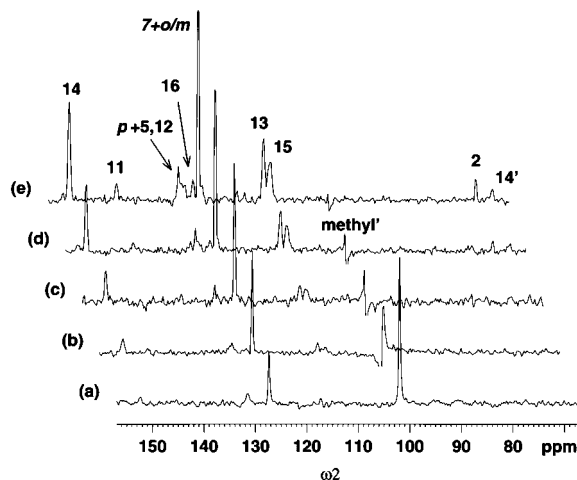


FIG. 5. The ω_2 slices of the 2D-RFDR experiment with different mixing times: (a) 16, (b) 32, (c) 48, (d) 64, and (e) 96 rotor cycles. The line at $\omega_2 = 102$ ppm is a spinning sideband of the ¹³C-labeled methyl carbon line at 20 ppm.

host carbon lines that did not overlap with the guest *p*-xylene resonances. Referring to the assignments made in Fig. 2, the peaks at 131.5 ppm and 127.5 ppm have contributions both from guest (*para* and *ortho/meta* carbons, respectively) and host (C12 and C7, respectively) carbons and therefore are not analyzed here. The strong line at 102 ppm in (a) is a spinning sideband of the labeled methyl spectrum. The lines we focused on were then those corresponding to C14, C11, C16, C13, C15, and C2. The MAS spectrum of C14 was the only one that showed a clear spinning sideband, marked by 14', in the ω_1 slice. No line intensities other than the diagonal peak of the guest methyl line ($\omega_1 = \omega_2$) were observed outside this spectral window.

As can be derived easily from Fig. 1, the ratio of guest to host molecules is 1:6. Since the guest molecules are labeled at only one of the two methyl positions in *p*-xylene, only half of the host carbons are “close” to a labeled methyl carbon. Thus only half of the NA ¹³C host carbons form isolated spin pairs with the labeled methyl carbons. The methyl ¹³C carbons are located on *C*₃ symmetry axes, relating three neighboring host molecule. The carbon–carbon distances between the ¹³C methyl carbons and the NA host carbons of the symmetry related molecules are therefore equal.

The 2D-RFDR TPPI experiments were recorded for various mixing times τ , and the ratios of the intensities of the cross-peak centerbands $F(\omega_1, \omega_2)$ to the diagonal peak centerbands $F(\omega_2, \omega_2)$ were plotted as function of τ , with ω_1 the isotropic chemical shift of the guest ¹³CH₃ carbons and ω_2 that of the host carbons. In order to account for half of the NA host carbons that do not experience a ¹³C-labeled guest carbon at their proximities, we subtracted half of the intensities of the diagonal centerbands at mixing time $\tau \approx 0$ from the intensities of all diagonal centerbands. Despite the π -pulses, the non-

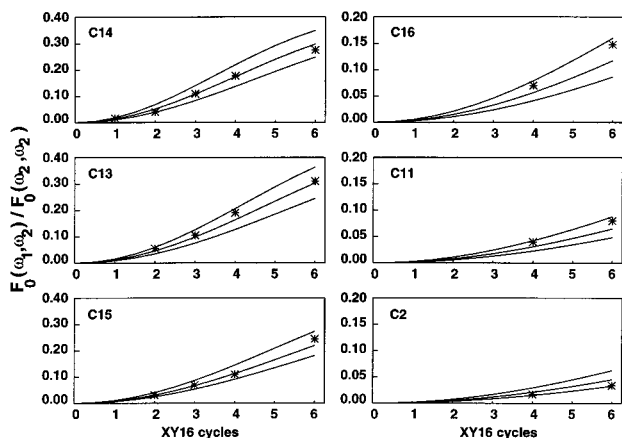


FIG. 6. Calculated versus experimental results of RFDR for different carbons in the host crystal of *p*-xylene/Dianin's compound. The experimentally measured ratio $F_0(\omega_1, \omega_2)/F_0(\omega_2, \omega_2)$, where ω_1 is the isotropic chemical shift of the guest-labeled CH_3 , and ω_2 the isotropic chemical shift of the host carbons (in the calculations, $\omega_1 = \Delta\omega$ and $\omega_2 = 0$). Solid lines represent simulations, asterisks experimental data. The lines were calculated for the distances given in Table 1 (middle line) and for overestimated (upper line) and underestimated (lower line) distance values. For host carbons C14, C15, and C13 the under-/overestimation was of $\pm 0.2 \text{ \AA}$, and for C16, C11, and C2, $\pm 0.3 \text{ \AA}$.

coupled carbon line intensities are maintained during the RFDR mixing time, due to the XY-16 phase cycling and the low rf pulse power.

The experimental results are shown in Fig. 6 and compared to the calculated values of the corresponding ratios $R(\tau, 0)/(1 - R(\tau, 0))$, according to Eq. [6]. For each host carbon the curves were simulated using the distances and CSA parameters in Table 1 as well as shorter and longer distances. As can be seen in Fig. 6, the results for the three host carbons (C14, C15, C13) within a distance of 4–5 Å from the labeled methyl guest carbon fall within a confidence interval of $\pm 0.2 \text{ \AA}$. For the smaller cross peaks corresponding to the three host carbons (C16, C11, C2) which are 5–6 Å away from the labeled methyl guest carbon, the results fall within a confidence interval of $\pm 0.3 \text{ \AA}$.

The fact that our sample is a singly ^{13}C labeled compound and that the density of carbons in Dianin's cage is low makes it reasonable to expect that the zero-quantum line broadening of the carbons in the pairs is very small. Thus in the analysis of the RFDR data we neglected the influence of T_2^{ZQ} .

CONCLUSIONS

We have applied the 2D-RFDR technique to measure distances of 4–6 Å in a singly labeled *p*-xylene/Dianin's inclusion compound. The effective dilution of the ^{13}C – ^{13}C spin pairs in this compound reduced the influence of T_2^{ZQ} on the data and allowed us to simulate the experimental results

without the evaluation of this relaxation effect. For the host carbons which are 4–5 Å away from the guest-labeled carbon, the resulting distances fall within $\pm 0.2 \text{ \AA}$ from the known distance, while for the host carbon 5–6 Å away, they fall within $\pm 0.3 \text{ \AA}$. The good agreement between the experimental and simulated results is an indication that the XY-16 phase cycling and the reduction of the RFDR pulse intensities were sufficient to eliminate the effects caused by pulse imperfections, off-resonance values, and undesired cross polarization on the data.

To generalize the 2D-RFDR approach for distance measurements, 2D spectra must be simulated, and the effect of the presence of sidebands must be studied for CSA tensors much larger than the spinning speed and dipolar interactions larger than 120 Hz. In addition, the numeric evaluation of the homonuclear linewidth, taking into account dipolar coupled multi-spin systems, is necessary to get a better estimate of the effect of T_2^{ZQ} on the experimental data.

ACKNOWLEDGMENT

This work was supported by a grant from the G.I.F., the German Israeli Foundation for Scientific Research and Development.

REFERENCES

1. R. R. Ernst, G. Bodenhausen, and A. Wokaun, "Principles of Nuclear Magnetic Resonance in One and Two Dimensions," Clarendon Press, Oxford (1987).
2. D. P. Raleigh, M. H. Levitt, and R. G. Griffin, *Chem. Phys. Lett.* **146**, 71–76 (1988).
3. M. H. Levitt, D. P. Raleigh, F. Creuzet, and R. G. Griffin, *J. Chem. Phys.* **92**, 6347 (1990).
4. R. Tycko and G. Dabbagh, *Chem. Phys. Lett.* **173**, 461–465 (1990).
5. A. E. Bennett, J. H. Ok, R. G. Griffin, and S. Vega, *J. Chem. Phys.* **96**, 8624–8627 (1992).
6. D. K. Sodickson, M. H. Levitt, S. Vega, and R. G. Griffin, *J. Chem. Phys.* **98**, 6742–6748 (1993).
7. T. Fujiwara, A. Ramamoorthy, K. Nagayama, K. Hioka, and T. Fujito, *Chem. Phys. Lett.* **212**, 81–84 (1993).
8. M. Baldus, M. Tomaselli, B. H. Meier, and R. R. Ernst, *Chem. Phys. Lett.* **230**, 329–336 (1994).
9. D. M. Gregory, D. J. Mitchell, J. A. Stringer, S. Kiihne, J. C. Shiels, J. Callahan, M. A. Mehta, and G. P. Drobny, *Chem. Phys. Lett.* **246**, 654–663 (1995).
10. B. Q. Sun, P. R. Costa, D. Kocisko, P. T. Lansbury, and R. G. Griffin, *J. Chem. Phys.* **102**, 702–707 (1995).
11. Y. K. Lee, N. D. Kurur, M. Helmle, O. G. Johannessen, N. C. Nielsen, and M. H. Levitt, *Chem. Phys. Lett.* **242**, 304–309 (1995).
12. T. Gullion and J. Schaefer, *J. Magn. Reson.* **81**, 196–200 (1989).
13. A. W. Hing, S. Vega, and J. Schaefer, *J. Magn. Reson.* **96**, 205–209 (1992).
14. B. Q. Sun, P. R. Costa, and R. G. Griffin, *J. Magn. Reson. A* **112**, 191–198 (1995).

15. J. M. Griffiths, K. V. Lakshmi, A. E. Bennett, J. Raap, C. M. Vanderwielen, J. Lugtenburg, J. Herzfeld, and R. G. Griffin, *J. Am. Chem. Soc.* **116**, 10178–10181 (1994).
16. P. R. Costa, B. Q. Sun, and R. G. Griffin, *J. Am. Chem. Soc.* **119**, 10821–10830 (1997).
17. A. E. Bennett, C. M. Rienstra, J. M. Griffith, W. Zhen, P. T. Lansbury, Jr., and R. G. Griffin, *J. Chem. Phys.* **108**, 9463–9479 (1998).
18. T. Gullion and S. Vega, *Chem. Phys. Lett.* **194**, 423–428 (1992).
19. P. Speier, G. Prigl, H. Zimmermann, U. Haeberlen, E. Zaborowski, and S. Vega, *Appl. Magn. Reson.* **9**, 81–102 (1995).
20. W. Baker, A. J. Floyd, J. F. W. McOmie, G. Pope, A. S. Weaving, and J. H. Wild, *J. Chem. Soc.*, 2010–2017 (1956).
21. P. Barker, N. E. Burlinson, B. A. Dunell, and J. A. Ripmeester, *J. Magn. Reson.* **60**, 486–489 (1984).
22. E. Zaborowski, S. Vega, P. Speier, H. Zimmermann, and U. Haeberlen, *Mol. Phys.* **91**, 1083–1096 (1997).
23. A. E. Bennett, C. M. Rienstra, M. Auger, K. V. Lakshmi, and R. G. Griffin, *J. Chem. Phys.* **103**, 6951–6958 (1995).
24. Y. Ishii, J. Ashida, and T. Terao, *Chem. Phys. Lett.* **246**, 439–445 (1995).
25. T. Gullion, D. B. Baker, and M. S. Conradi, *J. Magn. Reson.* **89**, 479–482 (1990).
26. T. M. Duncan, "A Compilation of Chemical Shift Anisotropies," The Farragut Press, Chicago (1990).
27. Y. Yang, A. Hagemeyer, K. Zemke, and H. W. Spiess, *J. Chem. Phys.* **93**, 7740–7750 (1990).
28. A. E. Bennett, R. G. Griffin, and S. Vega, Recoupling of homo- and heteronuclear dipolar interactions in rotating solids, in "NMR Basic Principles and Progress" (P. Diehl, E. Fluck, H. Gunther, R. Kosfeld, and J. Seelig, Eds.), Vol. 33, pp. 1–77, Springer-Verlag, Berlin (1994).
29. V. B. Cheng, H. H. Suzukawa, Jr., and M. Wofsborg, *J. Chem. Phys.* **59**, 3992–3999 (1973).
30. G. J. Boender and S. Vega, *J. Magn. Reson.* **133**, 281–285 (1998).